Letter Vol. 49, No. 1 / 1 January 2024 / Optics Letters 65

Microwave photonic I/Q mixer for wideband frequency downconversion with serial electro-optical modulations

Yuewen Zhou, Jiayuan Kong, Fangzheng Zhang,* and Shilong Pan

National Key Laboratory of Microwave Photonics, Nanjing University of Aeronautics and Astronautics, Nanjing 210016, China
**zhangfangzheng@nuaa.edu.cn*

Received 23 October 2023; revised 3 December 2023; accepted 3 December 2023; posted 4 December 2023; published 19 December 2023

In this paper, we propose a serial electro-optical (EO)-modulation-based microwave photonic in-phase and quadrature (I/Q) mixer and investigate its performance for wideband frequency downconversion. The proposed I/Q mixer uses two EO modulators and a programmable optical processor in a serially cascaded structure, which ensures good phase stability and flexibility to achieve high-performance broadband frequency downconversion. A proof-of-concept experiment is carried out in which the frequency downconversion of the RF signals in the range from 10 to 40 GHz is demonstrated with an average image rejection ratio of 38.66 dB. The spurious-free dynamic range (SFDR) measured at around 15 GHz is 86 dBc·Hz$^{2/3}$. Based on this microwave photonic I/Q mixer, a broadband radar receiver is established and de-chirping of linearly frequency modulated (LFM) radar echoes with an instantaneous bandwidth of 8 GHz (10–18 GHz) is achieved. The results verify its feasibility for high-performance I/Q mixing in practical applications.

https://doi.org/10.1364/OL.510130

In-phase and quadrature (I/Q) mixers are widely used in wireless communication, radar, and electronic warfare systems for signal reception [1–3], which can down convert a radio frequency (RF) signal to get a pair of intermediate frequency (IF) signals with quadrature phase. Traditional electrical I/Q mixers have difficulty maintaining good performance as the frequency or signal bandwidth increases. To address this problem, a number of microwave photonic I/Q mixing methods have been proposed and demonstrated, which have the potential for achieving high-performance frequency mixing with both a wide operation frequency range and a large signal bandwidth. In a typical microwave photonic I/Q mixer, a 90° phase difference is introduced between the optically carried RF and the local oscillator (LO) signals, which can be implemented by using an optical 90° hybrid or by leveraging the phase difference between the sidebands of different kinds of electro-optical (EO) modulations [4–7]. In these schemes, the RF and LO signals should be modulated onto an optical carrier in a parallel structure in which two independent optical channels including lasers, EO modulators and fiber links are essential. This would probably cause a phase interference to the I/Q mixing and result in the phase mismatch between I and Q channels because of the random phase change induced by fiber variation as well as the different characteristics of the EO modulators. Therefore, it is hard for these systems to fully play the role of photonic technologies.

In this Letter, we propose a microwave photonic I/Q mixer based on serial EO modulation and investigate its performance for wide-range frequency downconversion. Different from the previous microwave photonic I/Q mixing schemes, the proposed I/Q mixer is realized based on two serially connected EO modulators, through which EO conversions of the LO and RF signals are implemented in the same optical channel incorporating the modulators and fiber links. This way, the inconsistent modulation characteristics and phase unbalance problem can be avoided, and the phase stability is greatly enhanced. In addition, the proposed microwave photonic I/Q mixer uses a programmable optical processor (POP) to introduce the required phase difference between the two output channels. This brings the flexibility of regulating the phase relationship between the two output signals and provides a promising solution to high-precision and phase-reconfigurable mixing for variable applications.

Figure 1 shows the schematic diagram of the proposed microwave photonic I/Q mixer. Two laser diodes (LDs) generate two optical carriers at the frequencies of f_{c1} and f_{c2} ($f_{c1} < f_{c2}$), respectively. They are combined by an optical coupler (OC), and the combined optical signal is sent to a Mach–Zehnder modulator (MZM1) that is driven by the LO signal. By biasing the MZM1 at its quadrature transmission point, the output optical signal mainly contains the two optical carriers and their ±1st-order modulation sidebands. Here, the two optical carriers are separated by a large frequency spacing such that there is no spectral interference between the two electro-optically modulated optical signals. The obtained optical signal is sent to a POP, in which the amplitude and phase responses are properly programmed such that the two +1st-order modulation sidebands are blocked and the phase of the optical carrier at f_{c2} is rotated by 90°, as illustrated by the spectrum at point A in Fig. 1. The obtained optical signal can be expressed as

$$E_A(t) \propto J_0(\alpha)\cos(2\pi f_{c1}t) + J_1(\alpha)\sin[2\pi(f_{c1}-f_{LO})t] + J_0(\alpha)\sin(2\pi f_{c2}t) + J_1(\alpha)\sin[2\pi(f_{c2}-f_{LO})t], \quad (1)$$

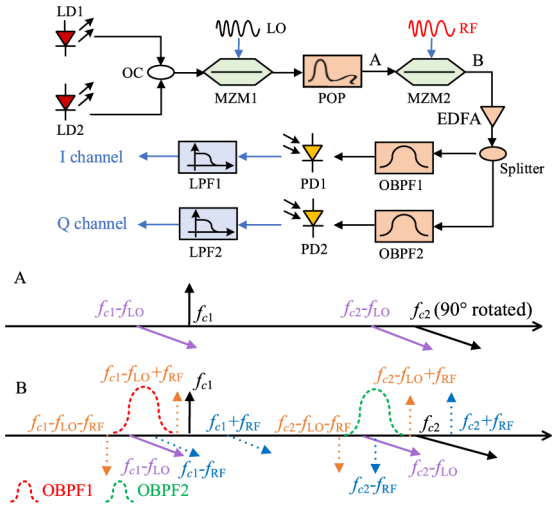

Fig. 1. Schematic diagram of the microwave photonic I/Q mixer.

where $J_p(\cdot)$ is the pth-order Bessel function of the first kind, α is the modulation index of MZM1, and f_{LO} is the frequency of the LO signal. Then, the output signal from the POP is fed into another MZM (MZM2), which is driven by the RF signal and biased at the quadrature transmission point. The output signal is mainly composed of the four frequency components in Eq. (1), and their $\pm 1^{st}$-order modulation sidebands, as indicated by the spectrum at point B in Fig. 1, in which the frequencies of the modulation sidebands are $f_{c1}-f_{LO}-f_{RF}$, $f_{c1}-f_{LO}$, $f_{c1}-f_{RF}$, $f_{c1}-f_{LO}+f_{RF}$, f_{c1}, $f_{c1}+f_{RF}$, $f_{c2}-f_{LO}-f_{RF}$, $f_{c2}-f_{LO}$, $f_{c2}-f_{RF}$, $f_{c2}-f_{LO}+f_{RF}$, f_{c2}, and $f_{c2}+f_{RF}$.

After MZM2, an erbium-doped fiber amplifier (EDFA) follows to compensate for the power loss, and the amplified optical signal is split into two branches with equal power by an optical splitter. In the upper branch, the signal is passed through an optical bandpass filter (OBPF1) to select out the frequency components at $f_{c1}-f_{LO}$ and $f_{c1}-f_{RF}$. Here, to avoid the spectral interference between the frequency components at $f_{c1}-f_{RF}$ and $f_{c1}-f_{LO}+f_{RF}$, $f_{LO}<2f_{RF}$ should be satisfied. The optical signal after OBPF1 is expressed as

$$E_I(t) \propto J_1(\alpha)J_0(\beta)\sin[2\pi(f_{c1}-f_{LO})t]+ J_0(\alpha)J_1(\beta)\sin[2\pi(f_{c1}-f_{RF})t], \quad (2)$$

where f_{RF} is the frequency of the RF signal and β is the modulation index of MZM2.

In the lower branch, the signal is passed through another optical bandpass filter (OBPF2) to select out the frequency components at $f_{c2}-f_{LO}$ and $f_{c2}-f_{RF}$, and the obtained signal is expressed as

$$E_Q(t) \propto J_1(\alpha)J_0(\beta)\sin[2\pi(f_{c2}-f_{LO})t]+ J_0(\alpha)J_1(\beta)\cos[2\pi(f_{c2}-f_{RF})t], \quad (3)$$

The optical signals in Eqs. (2) and (3) are sent to two photodetectors (PD1 and PD2), respectively, to implement photonic frequency mixing. The generated electrical signal after each PD is passed through a low-pass filter (LPF) to select out the frequency downconversion component at $f_{LO}-f_{RF}$. Assuming the two photodetectors have the same responsivity of R, the obtained two electrical signals in the two channels are given by

$$S_I(t) \propto RJ_0(\alpha)J_1(\alpha)J_0(\beta)J_1(\beta)\cos[2\pi(f_{LO}-f_{RF})t], \quad (4)$$

$$S_Q(t) \propto RJ_0(\alpha)J_1(\alpha)J_0(\beta)J_1(\beta)\sin[2\pi(f_{LO}-f_{RF})t], \quad (5)$$

in which R is the responsivity of the PDs.

Hitherto, the I/Q mixing for frequency downconversion is completed. The signals in Eqs. (4) and (5) are the in-phase and quadrature components of the frequency down-converted signal at $f_{LO}-f_{RF}$. In this system, EO conversions of the LO and RF signals, as well as the optical phase manipulation are implemented by two EO modulators and a POP that are serially connected by the same fiber link, which ensures the high phase stability required in high-performance I/Q mixing. In addition, the proposed method uses a POP to introduce the phase difference between I and Q channels, which is 90° in the previous deduction. In some applications, a phase difference other than 90° between the two output channels is required, e.g., the differential transmit scheme in [8] requires a phase difference of 180°. Since the POP used in our system can implement arbitrary phase rotation to a specific optical carrier, the proposed method can realize phase-reconfigurable frequency mixing to fit more applications.

To investigate the performance of the proposed microwave photonic I/Q mixer, a proof-of-concept experiment is carried out based on the setup in Fig. 1. Specifically, a multi-channel tunable laser (ID-photonics CoBrite-DX) is used to generate two optical carriers at 1550.12 and 1551.12 nm, respectively. Both of the two optical carriers have a power of 15 dBm, and they are combined by a 3 dB optical coupler. Two identical MZMs (iXblue MXAN-LN-40) having a 3 dB bandwidth of 40 GHz are used to implement electro-optical modulations. Two analog signal generators (R&S SMA100B) are applied to generate the LO signal and RF signal, respectively. The POP is a waveshaper (WS; Finisar Inc.) of which the minimum filter bandwidth can be set to 10 GHz, and the phase response can be controlled continuously in the range from 0 to 2π. After amplifying by an EDFA (Amonics, AEDFA-35-B-FA), the optical signal is equally split into two branches. In each branch, the OBPF (Yenista Optics Inc.) has a tunable center wavelength from 1450 to 1650 nm, the PD (Fby IA200) has a 3 dB bandwidth of 200 MHz and a responsivity of 0.90 A/W, and the LPF has a bandwidth of 80 MHz. The obtained I and Q channel signals are sampled by an oscilloscope (Agilent, DSO-X92504A) with a sampling rate of 5 GSa/s.

First, to verify the feasibility of the microwave photonic I/Q mixer, the LO and RF signals are set as single-tone signals at 15.05 and 15 GHz, respectively. Both of the two signals have a power of 10 dBm. Before implementing I/Q mixing, the phase response of the WS is calibrated and set to rotate 90° at the frequency of f_{c2}. The optical spectrum of the signal after the WS is measured by an optical spectral analyzer (OSA, YEC AQ6370D) with a resolution of 0.02 nm, as shown in Fig. 2, in which the signal contains two optical carriers and two -1^{st}-order modulation sidebands. When this optical signal

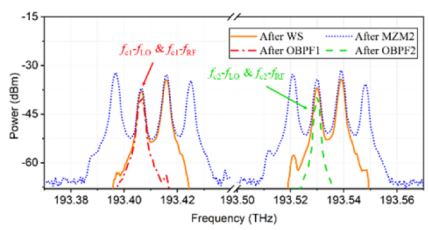

Fig. 2. Optical spectra measured after WS, MZM2, OBPF1, and OBPF2.

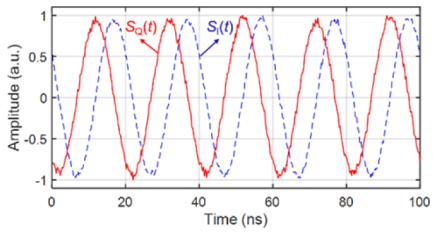

Fig. 3. Normalized waveforms of the I/Q signals.

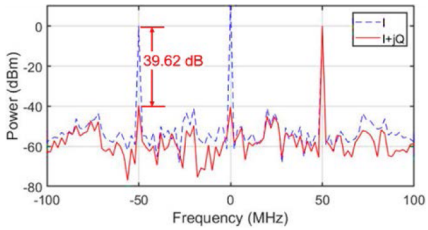

Fig. 4. Normalized spectra corresponding to the single-channel signal of $S_I(t)$ with a blue dash line and the complex signal of $S_I(t)+jS_Q(t)$ with a red line.

is modulated at MZM2 by the RF signal, the $\pm1^{st}$-order modulation sidebands are generated. Due to the limited resolution of the OSA, the frequencies in the four pairs of components at $(f_{c1}-f_{LO}, f_{c1}-f_{RF})$, $(f_{c1}-f_{LO}+f_{RF}, f_{c1})$, $(f_{c2}-f_{LO}, f_{c2}-f_{RF})$, and $(f_{c2}-f_{LO}+f_{RF}, f_{c2})$ cannot be distinguished, and thus eight spectral peaks are observed. When using two OBPFs to select out the frequency pairs of $(f_{c1}-f_{LO}, f_{c1}-f_{RF})$ and $(f_{c2}-f_{LO}, f_{c2}-f_{RF})$, respectively, the measured optical spectra are also shown in Fig. 2. After frequency downconversion, the signals in I and Q channels have the same frequency of 50 MHz, of which the normalized waveforms are shown in Fig. 3. By performing fast Fourier transformation (FFT) to the sampled I and Q channel signals and comparing the phases of the spectral components at 50 MHz, the phase difference between I and Q signals is calculated to be 89.45°, indicating the phase mismatch is 0.55°. Thus, the I and Q channels are close to ideal orthogonal signals. Then, the sampled I and Q signals are combined to obtain a complex signal of $S_I(t)+jS_Q(t)$. For comparison, the normalized frequency spectra corresponding to the single-channel signal of $S_I(t)$ and the complex signal of $S_I(t)+jS_Q(t)$ are calculated and shown in Fig. 4 with blue dash line and red line, respectively. It is found that the spectrum of $S_I(t)$ is symmetric about the zero frequency and two frequency components at 50 and −50 MHz are observed. Whereas, the spectrum of $S_I(t)+j\,S_Q(t)$ is single-sided and the image rejection ratio at −50 MHz is measured to be 39.62 dB. These results verify that the proposed microwave photonic I/Q mixer is successfully realized, which is capable of implementing the I/Q mixing for a single-tone signal with a high image rejection ratio.

Then, to investigate the operating frequency range of the microwave photonic I/Q mixer, the frequency of the RF signal is tuned from 10 to 40 GHz with a step of 1 GHz, and the bandpass of the WS is adjusted synchronously to select out the required optical frequency components. Here, the maximum RF frequency is determined by the 3 dB bandwidth of the MZM and the minimum RF frequency is set equal to the minimum filter bandwidth of the WS to ensure accurate amplitude and phase control. Meanwhile, the LO signal is also changed to be

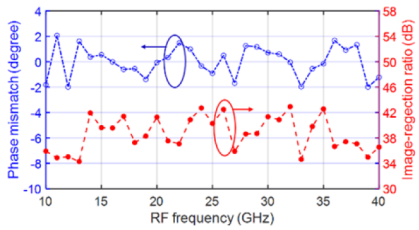

Fig. 5. Phase mismatch and image rejection ratio as a function of RF frequency.

50 MHz higher than the RF signal to make the down-converted I/Q frequencies lower than the LPF bandwidth. When tuning the frequencies of the RF and LO signals, the center frequencies of the OBPF1 and OBPF2 are adjusted to be $f_{c1}-(f_{LO}+f_{RF})/2$ and $f_{c2}-(f_{LO}+f_{RF})/2$, respectively. Based on the sampled signals, the phase mismatch between I and Q signals at each frequency is calculated and plotted in Fig. 5. As can be seen, the phase mismatch varies between ±2°, and the absolute average value is calculated to be 0.99°. Figure 5 also shows the image rejection ratio at −50 MHz measured through the spectrum of the complex signal $S_I(t)+jS_Q(t)$. In Fig. 5, the image rejection ratio keeps larger than 34 dB and is up to a maximum of 42.93 dB. The average image rejection ratio is calculated to be 38.66 dB. Compared with the parallel-modulation-based I/Q mixers demonstrated in [1,4,5], the established I/Q mixer achieves a smaller phase mismatch and a higher image rejection ratio in a large frequency range from 10 to 40 GHz. Therefore, the proposed I/Q mixer not only has the capability for broadband operation, but also has advantages in achieving a high image rejection ratio.

Next, the spurious-free dynamic range (SFDR) of the microwave photonic I/Q mixer is measured by mixing a dual-frequency RF signal and a single LO signal. The frequencies of the dual-frequency RF signal are 14.998 and 15 GHz, and the LO frequency and power remain to be 15.05 GHz and 10 dBm, respectively. The power of the fundamental component and the power of the third-order intermodulation distortion (IMD3) are measured at one output port of the I/Q mixer when the RF signal power is adjusted from −30 to 20 dBm with a step of 2 dB, as shown in Fig. 6, in which the noise floor is −67.7 dBm. In this process, the two frequency components have the same power, while the RF power is adjusted. Based on the measured results, quadric interpolations are implemented to obtain the two curves of the fundamental component power and the IMD3 power. It is found that, the third-order input intercept point (IIP3) is 31 dBm, and the SFDR of the microwave photonic I/Q mixer is 86 dBc·Hz$^{2/3}$. Thus, the proposed microwave photonic I/Q mixer is proved to have a good SFDR performance, which is significant for typical broadband signal reception.

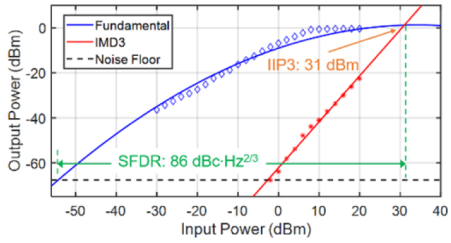

Fig. 6. Measured and interpolated output power of the fundamental component and the IMD3 component.

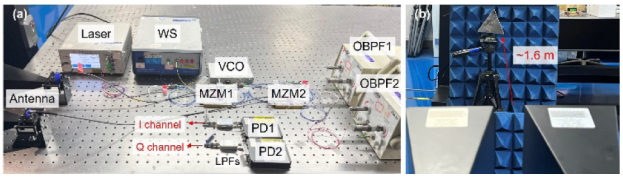

Fig. 7. Photograph of (a) the experimental setup of a microwave photonic I/Q mixing based radar system and (b) the detection scenario.

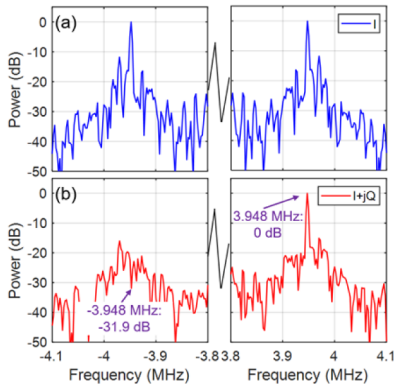

Fig. 8. Normalized spectra corresponding to (a) the single-channel de-chirped signal and (b) the complex de-chirped signal.

Finally, the microwave photonic I/Q mixer is applied in a radar receiver to investigate its performance for broadband radar de-chirping. Figures 7(a) and (b) show the detailed microwave photonic I/Q mixing based radar system and the detection scenario. The radar generates linear frequency modulated (LFM) signals using a voltage-controlled oscillator (VCO) having a frequency range of 10–18 GHz, a pulse width of 400 μs and an average power of 12 dBm. After equally splitting into two branches by a power splitter, one branch of the LFM signal is employed as the LO signal sent into MZM1, and the signal in the other branch is launched by a transmit antenna. The radar echoes are collected by a receive antenna and fed into MZM2. The bandpass of the WS and OBPFs are adjusted to select out the desired sidebands, while the phase response of the WS is still controlled to introduce a 90° phase rotation at the frequency of f_{c2}. The target is an angular reflector placed at the distance of ~1.6 m from the radar. After I/Q mixing, the wideband radar echoes are de-chirped to get a pair of low-frequency I and Q signals, which are sampled simultaneously with a sampling rate of 125 MSa/s. Figures 8(a) and (b) show the normalized frequency spectra corresponding to the single-channel de-chirped signal and the combined complex de-chirped signal, respectively. In Fig. 8(a), the target-related spectral peaks appear at the frequencies of ±3.948 MHz, based on which the target range is estimated to be 1.61 m. By combining the de-chirped I and Q signals, the frequency at −3.948 MHz is suppressed by 31.9 dB, as shown in Fig. 8(b). It should be noted that, the image rejection ratio for broadband radar de-chirping is slightly degraded compared with the results for I/Q mixing of single-tone signals shown in Fig. 5. This is partially due to the fact that the broadband LFM signal generated by a free-running electric VCO has an uneven amplitude envelope and a poor phase coherence between different pulses. In addition, the broadband scattering characteristics of nonideal point target leads to sidelobes around the rejected spectral notch, which also degrades the image rejection ratio. Nevertheless, the results can still verify the broadband I/Q mixing capability of the proposed microwave photonic I/Q mixer.

In conclusion, we have proposed and demonstrated a microwave photonic I/Q mixer that uses serial EO modulations to enhance the phase stability and improve the image rejection ratio. In the experiment, frequency downconversion of RF signals in the range from 10 to 40 GHz is achieved with an average image rejection ratio of 38.66 dB and an SFDR of 86 dBc·Hz$^{2/3}$ at around 15 GHz. The microwave photonic I/Q mixer is also proved to be capable in implementing broadband de-chirping of LFM radar echoes.

Funding. National Key Research and Development Program of China (2021YFB2800803); National Natural Science Foundation of China (62371224); Natural Science Foundation of Jiangsu Province (BK20221479); Fundamental Research Funds for the Central Universities (NS2023023); Postgraduate Research &Practice Innovation Program of Jiangsu Province (KYCX22_0362); Open Fund of State Key Laboratory of Advanced Optical Communication Systems and Networks (2023GZKF03).

Disclosures. The authors declare no conflicts of interest.

Data availability. Data underlying the results presented in this Letter are not publicly available at this time but may be obtained from the authors upon reasonable request.

REFERENCES

1. Z. Meng, J. Li, C. Yin, *et al.*, Opt. Express **25**, 22055 (2017).
2. H. Emami and N. Sarkhosh, J. Opt. Soc. Am. A **31**, 1320 (2014).
3. X. Ye, F. Zhang, Y. Yang, *et al.*, Photonics Res. **7**, 265 (2019).
4. J. L. Jianqiang Li, J. X. Jia Xiao, X. S. Xiaoxiong Song, *et al.*, Chin. Opt. Lett. **15**, 010014 (2017).
5. J. Shi, F. Zhang, D. Ben, *et al.*, J. Lightwave Technol. **36**, 4319 (2018).
6. Y. Gao, H. Chi, J. Dai, *et al.*, Opt. Express **31**, 2135 (2023).
7. B. Kang, Y. Fan, W. Wang, *et al.*, Opt. Commun. **456**, 124579 (2020).
8. T. Himsoon, W. F. Su, and K. J. R. Liu, IEEE Trans. Signal Process. **54**, 3305 (2006).